



## Preparation of Aligned Porous Ni-GDC Nano Composite by Freeze-Casting Process

Z. Khakpour<sup>\*a</sup>, A. Mousavi<sup>a</sup>, M. Niazmand<sup>a</sup>, M. Alizadeh<sup>a</sup>, A. Zamanian<sup>b</sup>

<sup>a</sup>Department of Ceramic Engineering, Materials and Energy Research Center, Karaj, Iran

<sup>b</sup>Department of Nanomaterials and Advanced Materials, Materials and Energy Research Center, Karaj, Iran

### PAPER INFO

#### Paper history:

Received 17 January 2017

Accepted in revised form 16 May 2017

#### Keywords:

Ni-GDC composite  
Gel-combustion  
Freeze casting  
Pore structure

### ABSTRACT

This study reports preparation of Nickel-Gadolinium doped Ceria (Ni-GDC) composite via controlled unidirectional freeze casting of aqueous-based GDC slurry completed with nickel infiltration into the porous GDC samples. Gadolinium doped ceria powder was prepared by gel-combustion synthesis method. The oxide powder was confirmed by X-ray diffraction to be the fluorite-structured of  $Ce_{0.8}Gd_{0.2}O_{1.9}$  solid solution. The synthesized powder was used with dolapix as a dispersant, Ammonia solution as an agent pH, poly vinyl alcohol (PVA) as a binder and water as a solvent to prepare stable GDC slurries. Freeze casting process was done in different solid loadings of GDC at 35, 45 and 55 wt. %, and two different cooling rates of 1 and 3 °C/min to obtain desirable pore structure. After removing the frozen ice at -58 °C, the green samples were sintered for 2 h in air at 1300 °C. The pore structure and final microstructure were studied by scanning electron microscopy. The porosity of the sintered samples was in range of 60-70% , and depended on solid content and freeze casting rate. Finally, nickel solution was infiltrated into the hierarchically porous GDC samples, after reduction at 800 °C, Ni-GDC composite was attained.

## 1. INTRODUCTION

Fuel cells have attracted considerable attention as these electrochemical devices can directly convert chemical energy to electrical energy. Performance of all type of fuel cells depends on performances of their components that includes: electrolyte, anode, cathode, and interconnect [1]. Among fuel cells, solid oxide fuel cells (SOFCs) components are solid ceramic materials and due to ionic conductivity of ceramic electrolytes at intermediate temperatures, SOFCs operate at extremely high temperatures (600–1000°C) [2]. Although, SOFCs have been the most fuel efficient fuel cells, their high operating temperature leads to high costs of interconnectors and other construction materials and also they have short lifetimes. Then there have been many efforts for investigating and finding ways to decrease the operating temperature to obtain low cost SOFCs. Achieving low operating temperature will therefore allow the use of low-cost and widely commercially available materials such as stainless steel for interconnecting and structural components [2-4]. Consequently, current research efforts are aimed at improving components performance at intermediate

temperatures or less. Yttria-stabilized zirconia (YSZ) is the most common electrolyte in SOFCs [5] but because of the lower ionic conductivity of the YSZ solid electrolyte at lower operating temperatures, replacement of YSZ by Ceria based materials that have higher ionic conductivity at intermediate temperature is preferred.  $Gd^{3+}$  doped  $CeO_2$  (GDC) is considered to be one of the most promising electrolytes for intermediate temperature SOFCs (IT-SOFCs) [6]. In order to achieve the purpose of reducing operation temperature both high conductivity and microstructural characteristics of the electrodes are essential [7]. The suitable anode for GDC electrolyte-based SOFCs is thought to be Ni-GDC cermets [7,8]. The main functions of the anode could be broadly classified as to provide (i) reaction sites for the electrochemical oxidation of the fuel, and (ii) a path for electrons to be transported from the reaction sites to the interconnect. Sufficient amount of porosities is necessary to allow the fuel and byproducts to be delivered and removed from the reaction sites without significant diffusion limitation [9,10]. Various methods have been applied for synthesis and fabrication of composite SOFCs anode. Tape casting method for making anodes resulted in porous structure in which porosity decreases with increasing sintering temperature [11]. Freeze casting method for the fabrication of Ni-GDC anode material has not been studied. Hag Koh et

\*Corresponding Author's Email: [z-khakpour@merc.ac.ir](mailto:z-khakpour@merc.ac.ir) (Z.Khakpour)

al. [12] used freeze-casting technique to fabricate Ni-YSZ cermets. The samples were sintered at temperatures of 1100 to 1400° C, and finally sintered samples were kept at temperatures of 600 to 900° C in argon/hydrogen atmosphere. In another similar study, NiO-YSZ anode was fabricated by freeze casting method which was frozen at -30° C and after drying and sublimation of ice, the samples was obtained as a tablet with a diameter of 5.2cm [13].

The freeze-casting technique to produce porous Ni-GDC anode has not been used yet and the present study is the first attempt to prepare it with via method. After preparing porous GDC samples, nickel was impregnated to them. The variable suspension concentration, freeze-casting and the cooling rate in final sintering temperature and its effects on microstructure generated were reviewed.

## 2. EXPERIMENTAL

### 2.1. Fabrication procedure

To prepare a Ni-GDC nanocomposite, at first step  $Gd_{0.2}Ce_{0.8}O_{1.9}$  (GDC) nanopowder was synthesized via the sol-gel combustion.  $Ce(NO_3)_3 \cdot 6H_2O$  (99.99%, Merck),  $Ni(NO_3)_2 \cdot 6H_2O$  (99.99%, Merck),  $Gd(NO_3)_3 \cdot 6H_2O$  (99.99%, Aldrich) and Citric Acid (99 % Merck) were used as the starting materials.  $Ce(NO_3)_3 \cdot 6H_2O$  and  $Gd(NO_3)_3$  were mixed and dissolved in distilled water. Citric Acid as a complex ion agent was dissolved in distilled water and then added to the mixture of the primer solution. After homogenizing the solution, temperature was raised to 80°C and maintained under stirring condition to remove the excess water to obtain a transparent gel. The molar ratio of citric acid to the cations of solution was 3. The obtained transparent gel-like material was then combusted at 150°C for 10 h, and the gaseous products such as  $N_2$ ,  $CO_2$  and  $H_2O$  were removed as the byproducts. Then, the as combusted yellowish ash was calcined in a furnace at 800°C for 2 h to obtain a completely crystalline nanocomposite powder.

Next, porous GDC samples were prepared by unidirectional freeze-casting method from stable slurries of synthesized GDC powder. For this purpose, a polyelectrolyte dispersant (Dolapix CE 64, Zschimmer & Schwarz, Lahnstein, Germany) which is commercially available, was used as a dispersant for powder dispersion. The sedimentation experiments were conducted by adjusting the dispersant concentration. The slurries were stored in a glass graded and placed in a water bath for ultrasonication for 15 min to break up the soft agglomerates. Then the slurries were allowed to settle and the sedimentation was recorded. In following, an optimum amount of Dolapix was added to distilled water according to sedimentation results, then polyvinyl alcohol (PVA, Mw = 15000, Merck, Darmstadt, Germany) as a binder and GDC powder

were also gradually added, and the process was followed by stirring at 1000 rpm for 1 h. The pH of the slurry was adjusted to 12 (the zeta potential was determined with a Zetasizer 3000 HAS) by the gradual addition of a 1 M ammonia solution. Before conducting the freeze-casting process, the prepared slurries were kept in a vacuum oven for 30 min at a pressure of 0.02 MPa to eliminate air bubbles. After that, slurries were poured into a PTFE mold (20 mm diameter). The mold was placed on copper, where the temperature was controlled by using liquid nitrogen and a ring heater was connected to a PID controller. The cooling rates used in this study were chosen as 1 and 3 °C/min in the axial direction of the samples. After casting, frozen samples were carefully demoulded and transferred into a freeze dryer. The sublimation was carried out in the freeze dryer at the temperature of -58°C and pressure of 2.1 Pa. For sintering, the green bodies were heated at 5°C/min to the desired temperature (1300 °C) and held isothermally for 2 h. Finally, Nickel ions were infiltrated into porous GDC bodies from 2 molar nickel nitrate solution. After reducing at 800° C in a hydrogen stream at the rate of 100 ml min<sup>-1</sup> for 2 h, Ni-GDC cermets anodes were obtained.

### 2.2. Characterization

The phase compositions of the as synthesized ash, calcined GDC powders, and the sintered GDC pellets were studied by X-ray diffractometer (Philips) using Cu K $\alpha$  radiation ( $\lambda = 1.5 \text{ \AA}$ ) and Co K $\alpha$  radiation ( $\lambda = 1.7 \text{ \AA}$ ) as X-ray source, with step size of 0.02° and a step time of 2 s. Thermogravimetric analysis (TGA) and differential thermal analysis (DTA) were performed by using NETZSCH STA 409 PC /PG thermoanalyzer in an air atmosphere at heating rate of 5 °C/min. For determining bulk density, the weight and the bulk volume of the sintered samples were measured and  $d_b$  was calculated as shown in Eq. (1):

$$d_b = \frac{m}{V} \quad (1)$$

Where  $d_b$  is bulk density (g/cm<sup>3</sup>), m is weight of the sample (g) and V is the bulk volume (cm<sup>3</sup>). The following equation was used to determine the porosity (Pt):

$$P_t = 100 \left( 1 - \frac{d_b}{d_t} \right) \quad (2)$$

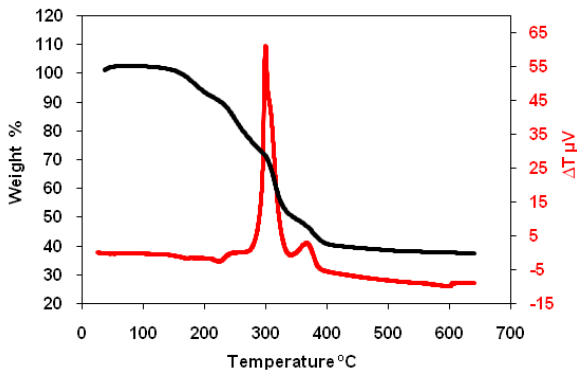
Where  $D_t$  is the theoretical density of the powder.

Morphology of the powder and sintered samples was evaluated by field emission scanning electron microscopy (FE-SEM, ZEISS) equipped with energy dispersive spectrometer (EDS).

## 3. RESULT AND DISCUSSION

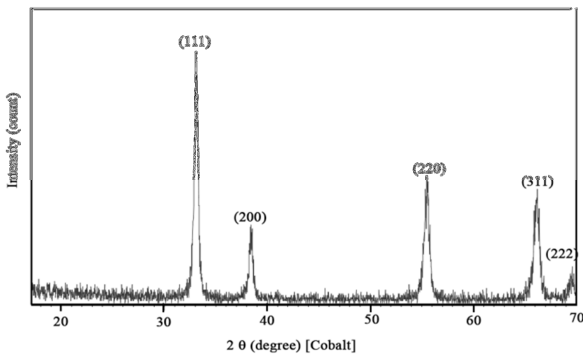
Thermal reactions of dried gel which was synthesized through sol-gel combustion includes removing of water,

combustion of organic materials and crystallization [14]. Fig. 1 shows simultaneous TGA and DTA curves of the synthesized GDC powder. It can be seen that thermal reactions are conducted with about 60% weight reduction. The 10% weight loss up to 200° C in TG curve corresponds to removal of water in the gel precursor. Weight loss in the temperature range from 200 to 400° C is about 50 % which is accompanied with strong exothermic peak in DTA curve which can be observed at 300° C and another exothermic peak at 370° C is related to combustion reaction, burning out of organic materials and the oxidation of the chelating complex along with the formation of metal oxides.



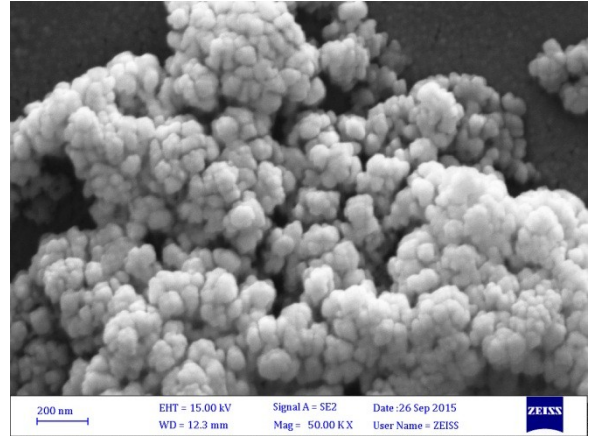
**Figure 1.** TG/DTA curves of the gel-combustion GDC nano powder.

Fig. 2 shows the XRD pattern of the synthesized GDC powders after calcinations at 850° C, formation of the GDC phase was confirmed for the powder according to JCPDS file nos.75-0162 and no other phases could be found within the sensitivity of XRD. Fig. 3 shows the typical morphology of the synthesized powder, consisting of homogenous and weakly agglomerated particles with approximate size of 40–150 nm.



**Figure 2.** XRD patterns of the calcinated synthesized GDC nano powder at 850° C.

Stability of the GDC suspension was measured with dolapix as a dispersant in terms of changes of sediment volume as a function of dolapix and time.



**Figure 3.** SEM image of GDC nano powder which was synthesized via gel combustion method.

Fig. 4 shows the effect of dispersant percent on the sedimentation volume of slurries. As it can be seen, the slurry at 3 wt.% dolapix was able to sustain with approximate 25% loss of sedimentation volume for more than 72 hours. The effect of pH on the sedimentation volume of slurries with dispersant was considered by zeta potential measurement (Fig. 5). As it can be seen in Fig. 5, for the suspension containing 3 wt.% dolapix, the zeta potential exceeded the 30 mV in the pH range of 10 and the maximum zeta potential was greater than 40 mV which was obtained in pH= 12. According to zeta potential and sedimentation results, 3 wt.% dolapix was used for the preparation of freeze casting slurry and the slurry was kept at pH 12.

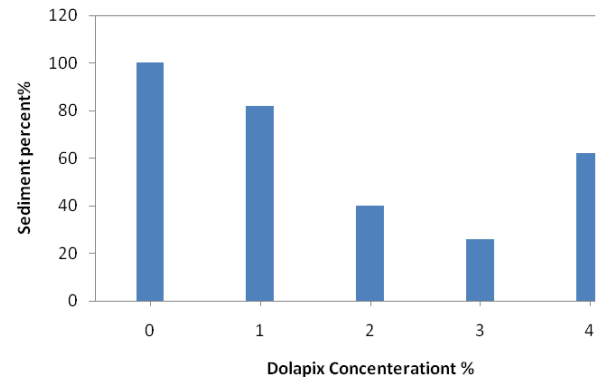


**Figure 4.** Sediment percent as a function of dispersant concentration.

Freeze casting aqueous solutions requires green densities in excess of 50% green density and solids loading in excess of 55 wt.% solids to achieve dense ceramic bodies [15]. Therefore, the freeze casting was employed in GDC slurries in solid loadings of 35, 45 and 55 wt.% in order to form significant porosity. The produced freeze-cast composites displayed two distinct levels of porosity: macropores which were resulted from the sublimation of the aligned ice crystals and

microporosity in the walls of the macro pores [16]. Fig. 6, shows microstructures of the surface (horizontal section) of the sintered bodies along with varying the loading.

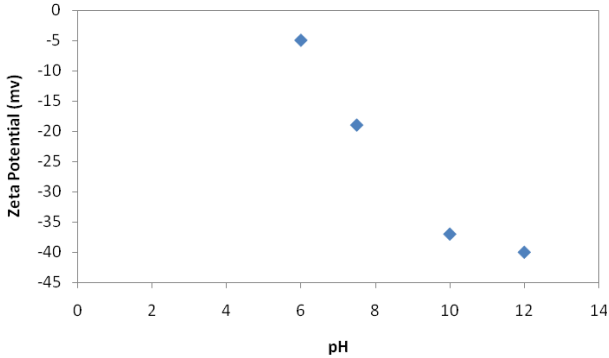


**Figure 5.** Effects of pH value on zeta potential of the solution containing 3 wt.% Dolapixas dispersant.

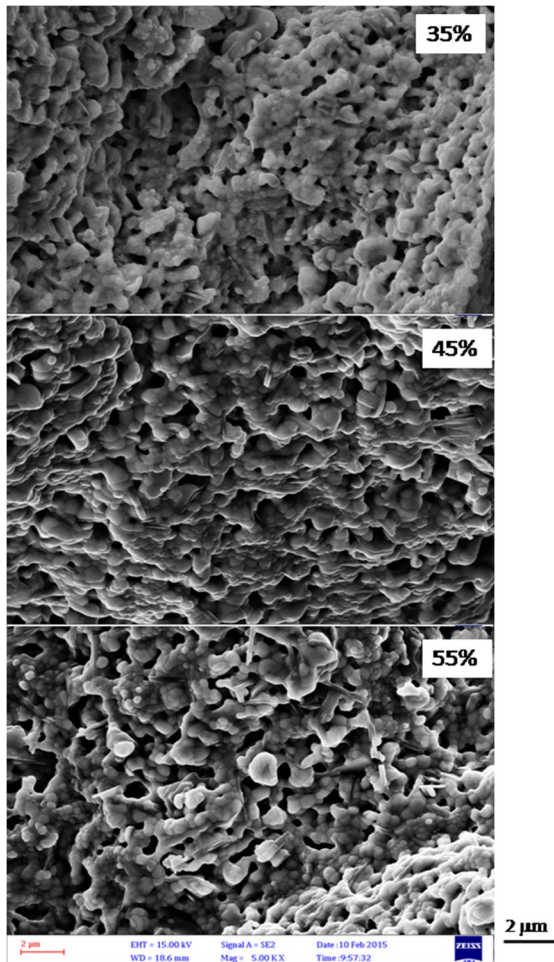


**Figure 6.** SEM micrographs of surface of sintered porous ceramics prepared by different (35, 45, and 55) wt.% solid loading suspensions.

According to the Fig. 6, open pores are obvious at the surface between grains but alignment of the pores could

not be seen at this section, so microstructure of vertical cross section of these samples are shown in Fig. 7. The columnar pores which were grown perpendicular to the freezing platen, are evident in all three samples, but with increasing the solid loading up to more than 35%, pore width was decreased and thickness of the lamellae was increased. In 35% solid loading sample, bridge is formed between the lamella layers, and by increasing solid loading redistribution of the particles during solidification becomes more tough and the ice crystals will engulf the ceramic particles rather than pushing them aside therefore smaller pore width and lamella spaces are formed in 45 % and 55% samples.

The green and sintered porosity of porous freeze cast GDC samples with the sintering shrinkage in different solid loadings are listed in Table 1. Very high porosity (69%) is obtained in the samples which were processed with 35 wt.% solids; however, increasing the solid loading could not changed the porosity of specimens significantly which is in disagreement with some other reports [17]. According to some references, porosity levels of partially sintered freeze-casts varied approximately linearly with initial solid loading for all samples regardless of freezing rate or viscosity [17-20]. This exceptional phenomenon in our study can be explained by decrease in shrinkage which was observed by increasing the solid loading as shown in Table 1.

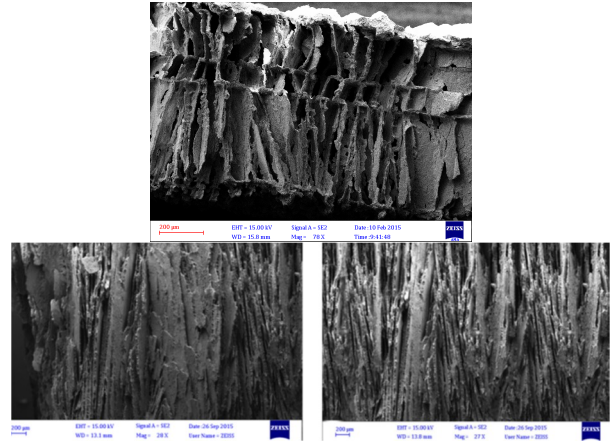


**Figure 7.** SEM micrographs of vertical section of sintered porous ceramics prepared by 35 (top), 45 (right) and 55wt.% solid loading suspensions.

**TABLE 1.** Physical properties of freeze casting samples.

Solid loading (%)	porosity (%) of green compact	porosity (%) of sintered compact	Shrinkage
35	75	70	11.34
45	71	64	9.34
55	68	60	7.9

Since the GDC powder that was used in this study was in the range of nanometer sizes, agglomeration of the powder could affect densification during sintering process, therefore, in spite of changes in pore width and lamella shapes (Fig. 7) there are small differences in total porosity level of the samples. According to D. Koch et al. [21, 22], the state of porosity is hardly changed from the green microstructure when the sintering temperature is restricted to 1100 °C in alumina bodies and higher temperatures lead to volume shrinkage and increase the average pore sizes. In our study, sintering temperature was 1300° C, and more study on sintering temperature now is in process. The pore size can be modified mostly by increasing or decreasing the cooling rate of the cold finger during the freezing [17-22]. For low cooling rate in the range of 1° C/min, the final microstructure will be characterized by large lamellae thickness (>50 μm) and pore width (>100 μm min) in 55% solid loading sample (Fig. 7). Conversely, for fast cooling rate (3 °C/ min), tiny lamellae (> 30 μm) and pore width (70 μm) are obtained.

Specimens with porosity minimum solid loading do not provide the level of structural support needed for anode at anode supported fuel cells, Therefore, the sample with an initial concentration of 45 vol.% GDC and a cooling rate of 3 °C/min along with porosity of 64 %, and pore width of 50 μm was determined for Ni infiltration process. Fig. 8, shows XRD pattern of Ni-GDC nano-composite materials which was derived from the porous freeze-casting GDC sample.

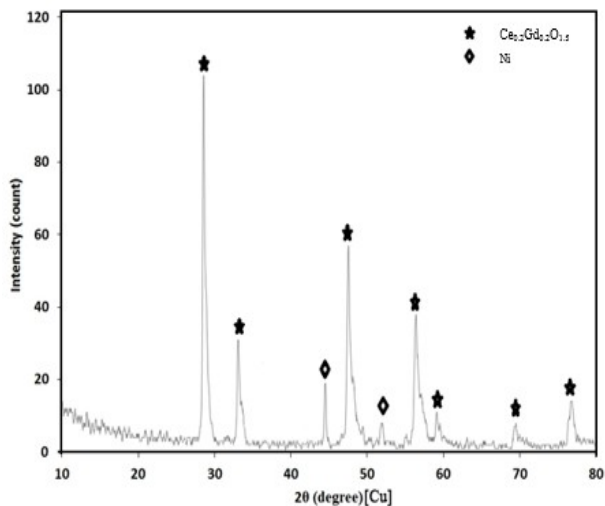


**Figure 8.** XRD patterns of prepared Ni-GDC composite after reduction at 800°C and keeping in a hydrogen stream.

Nickel nitrate solution was infiltrated to the porous sample, after sintering and reduction by keeping sample in hydrogen stream at 800° C, for which, XRD analysis indicated the diffraction peaks relating to GDC and Ni metal crystal phases. SEM images of the NiO-GDC

pellets prepared by sintering the Ni infiltrated porous freeze casting GDC sample are shown in Fig. 9. The open porosities of the GDC sample prepared via freeze casting method have attained a suitable porous structure for Ni diffusion. In fact, the fabricated cermet anode contains sufficient porosity which is an important factor for creating high density TPBs, which acts as the electrochemically active sites for the electrode reactions [23-25]. Therefore, freeze casting porous anode can be considered as an appropriate material for effective application in SOFCs. Complementary study in this area is progress.

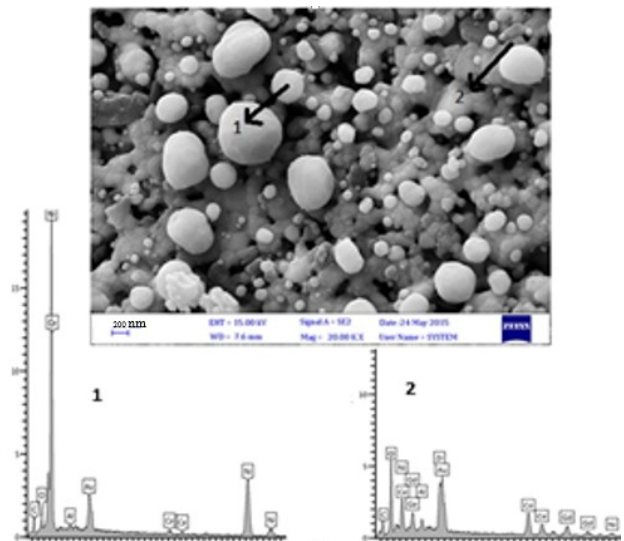


**Figure 9.** SEM image and elemental analysis of Ni-GDC composite anode after reduction at 800°C, Nickel particles are shown by arrows in the picture.

#### 4. CONCLUSION

The objective of this work was to develop porous ceramic GDC material with total porosity of 60-70% by freeze-casting process followed by the infiltration of Ni to obtain Ni-GDC anode. Results indicated that freeze casting of GDC nanopowder slurry results open and unidirectional aligned pores, and the porosity of the samples was increased from 60% to 70% when the solid loading was decreased from 55 to 35 wt.%.

#### 5. ACKNOWLEDGMENTS

The authors would like to acknowledge the financial support of Materials & Energy Research Center of Iran for this research.

#### REFERENCES

1. Kuang, K. and Easler, K., Fuel cell electronics packaging, (2007).
2. Stambouli, A.B. and Traversa, E., "Solid oxide fuel cells (SOFCs): a review of an environmentally clean and efficient

- source of energy", *Renewable and Sustainable Energy Reviews*, Vol. 6, No. 5, (2002), 433-455.
3. Singhal, S. and Kendall, K., "High Temperature Solid Oxide Fuel Cells: Fundamentals, Design and Applications", Elsevier Science, (2004).
  4. O'Hayre, R., Cha, S.W., Colella, W. and Prinz, F.B., "Fuel cell fundamentals", New York: John Wiley & Sons, (2006), 1-8.
  5. Minh, N.Q., Minh, N. Q., "Ceramic fuel cells", *Journal of the American Ceramic Society*, Vol. 76, No. 3, (1993), 563-588.
  6. Steele, B.C.H., "Appraisal of  $Ce_{1-y}Gd_yO_{2-y/2}$  electrolytes for IT-SOFC operation at 500°C", *Solid State Ionics*, Vol. 129, (2000), 95.
  7. Xia, C. and Liu, M., "Microstructures, conductivities, and electrochemical properties of  $Ce_{0.9}Gd_{0.1}O_2$  and GDC-Ni anodes for low-temperature SOFCs", *Solid State Ionics*, Vol. 152, (2002), 423-430.
  8. Gil, V., Tartaj, J. and Moure, C., "Chemical and thermomechanical compatibility between Ni-GDC anode and electrolytes based on ceria", *Ceramics International*, Vol. 35, (2009), 839-846.
  9. Setoguchi, T., Okamoto, K., Eguchi, K. and Arai, H., "Effects of anode material and fuel on anodic reaction of solid oxide fuel cells", *Journal of the Electrochemical Society*, Vol. 139, No. 10, (1992), 2875-2880.
  10. Suddhasatwa, B., "Recent trends in fuel cell science and technology", Springer New York, (2007), 157-187.
  11. Fu, C., Chan, S.H., Liu, Q., Ge, X. and Pasciak, G., "Fabrication and evaluation of Ni-GDC composite anode prepared by aqueous-based tape casting method for low-temperature solid oxide fuel cell", *International Journal of Hydrogen Energy*, Vol. 35, No. 1, (2010), 301-307.
  12. Koh, Y.H., Sun, J.J. and Kim, H.E., "Freeze casting of porous Ni-YSZ cermets", *Materials Letters*, Vol. 61, No. 6, (2007), 1283-1287.
  13. Gannon, P., Sofie, S., Deibert, M., Smith, R. and Gorokhovskiy, V., "Thin film YSZ coatings on functionally graded freeze cast NiO/YSZ SOFC anode supports", *Journal of Applied Electrochemistry*, Vol. 39, No. 4, (2009), 497-502.
  14. Karaca, T., Altınçekiç, T.G. and Öksüzömer, M.F., "Synthesis of nanocrystalline samarium-doped  $CeO_2$  (SDC) powders as a solid electrolyte by using a simple solvothermal route", *Ceramics International*, Vol. 36, No. 3, (2010), 1101-1107.
  15. Sofie, S.W., "Fabrication of Functionally Graded and Aligned Porosity in Thin Ceramic Substrates With the Novel Freeze-Casting Process", *Journal of the American Ceramic Society*, Vol. 90, No. 7, (2007), 2024-2031.
  16. Lichtner, A.Z., Jauffres, D., Martin, C.L. and Bordia, R.K., "Processing of Hierarchical and Anisotropic Porosity LSM-YSZ Composites", *Journal of the American Ceramic Society*, Vol. 96, No. 9, (2013), 2745-2753.
  17. Deville, S., "Freeze-casting of porous ceramics: a review of current achievements and issues", *Advanced Engineering Materials*, Vol. 10, No. 3, (2008), 155-169.
  18. Araki, K. and Halloran, J.W., "Porous ceramic bodies with interconnected pore channels by a novel freeze casting technique", *Journal of the American Ceramic Society*, Vol. 88, No. 5, (2005), 1108-1114.
  19. Deville, S., Saiz, E. and Tomsia, A.P., "Freeze casting of hydroxyapatite scaffolds for bone tissue engineering", *Biomaterials*, Vol. 27, No. 32, (2006), 5480-5489.
  20. Farhangdoust, S., Zamanian, A., Yasaei, M. and Khorami, M., "The effect of processing parameters and solid concentration on the mechanical and microstructural properties of freeze-casted macroporous hydroxyapatite scaffolds" *Materials Science and Engineering: C*, Vol. 33, No. 1, (2013), 453-460.
  21. Koch, D., Andresen, L., Schmedders, T. and Grathwohl, G., "Evolution of porosity by freeze casting and sintering of sol-gel derived ceramics", *Journal of sol-gel science and technology*, Vol. 26, No. (1-3), (2003), 149-152.
  22. Liu, G. and Button, T.W., "The effect of particle size in freeze casting of porous alumina-zirconia composite", *Ceramics International*, Vol. 39, No. 7, (2013), 8507-8512.
  23. Ishihara, T., Shibayama, T., Nishiguchi, H. and Takita, Y., "Nickel-Gd-doped  $CeO_2$  cermet anode for intermediate temperature operating solid oxide fuel cells using  $LaGaO_3$ -based perovskite electrolyte", *Solid State Ionics*, Vol. 132, No. 3, (2000), 209-216.
  24. Moon, H., Kim, S.D., Hyun, S.H. and Kim, H.S., "Development of IT-SOFC unit cells with anode-supported thin electrolytes via tape casting and co-firing", *International Journal of Hydrogen Energy*, Vol. 33, No. 6, (2008), 1758-1768.
  25. Nagamori, M., Shimonosono, T., Sameshima, S., Hirata, Y., Matsunaga, N., Sakka, Y., "Densification and Cell Performance of Gadolinium-Doped Ceria (GDC) Electrolyte/NiO-GDC anode Laminates", *Journal of the American Ceramic Society*, Vol. 92, No. 1, (2009), 117-121.